



The Holy Grail of Resource Assessment: Low Cost Ground-Based Measurements with Good Accuracy

Preprint

Bill Marion

National Renewable Energy Laboratory

Benjamin Smith

Enphase Energy

*Presented at the 2017 IEEE Photovoltaic Specialists Conference
Washington, DC*

June 25–30, 2017

© 2018 IEEE. Personal use of this material is permitted. Permission from IEEE must be obtained for all other uses, in any current or future media, including reprinting/republishing this material for advertising or promotional purposes, creating new collective works, for resale or redistribution to servers or lists, or reuse of any copyrighted component of this work in other works.

**NREL is a national laboratory of the U.S. Department of Energy
Office of Energy Efficiency & Renewable Energy
Operated by the Alliance for Sustainable Energy, LLC**

This report is available at no cost from the National Renewable Energy Laboratory (NREL) at www.nrel.gov/publications.

Conference Paper
NREL/CP-5J00-67806
August 2018

Contract No. DE-AC36-08GO28308

NOTICE

This work was authored by the National Renewable Energy Laboratory, operated by Alliance for Sustainable Energy, LLC, for the U.S. Department of Energy (DOE) under Contract No. DE-AC36-08GO28308. Funding provided by the U.S. Department of Energy's Office of Energy Efficiency and Renewable Energy (EERE), Solar Energy Technologies Office. The views expressed in the article do not necessarily represent the views of the DOE or the U.S. Government. The U.S. Government retains and the publisher, by accepting the article for publication, acknowledges that the U.S. Government retains a nonexclusive, paid-up, irrevocable, worldwide license to publish or reproduce the published form of this work, or allow others to do so, for U.S. Government purposes.

This report is available at no cost from the National Renewable Energy Laboratory (NREL) at www.nrel.gov/publications.

U.S. Department of Energy (DOE) reports produced after 1991 and a growing number of pre-1991 documents are available free via www.osti.gov.

Cover Photos by Dennis Schroeder: (left to right) NREL 26173, NREL 18302, NREL 19758, NREL 29642, NREL 19795.

NREL prints on paper that contains recycled content.

The Holy Grail of Resource Assessment: Low Cost Ground-Based Measurements with Good Accuracy

Bill Marion¹, Benjamin Smith²

¹National Renewable Energy Laboratory, Golden, CO, USA

²Enphase Energy, Inc., Petaluma, CA, USA

Abstract — Using performance data from some of the millions of installed photovoltaic (PV) modules with micro-inverters may afford the opportunity to provide ground-based solar resource data critical for developing PV projects. The method used back-solves for the direct normal irradiance (DNI) and the diffuse horizontal irradiance (DHI) from the micro-inverter ac production data. When the derived values of DNI and DHI were then used to model the performance of other PV systems, the annual mean bias deviations were within $\pm 4\%$, and only 1% greater than when the PV performance was modeled using high quality irradiance measurements. An uncertainty analysis shows the method better suited for modeling PV performance than using satellite-based global horizontal irradiance.

Index — direct and diffuse irradiance, performance, model, micro-inverter.

I. INTRODUCTION

Ground-based solar resource measurements are critical for developing PV projects. Unfortunately, accurate measurements at most locations are lacking due to the cost of solar radiation measurement equipment, which can be more than \$40,000 for a first class station. In order to provide low or no-cost solar resource data traceable to a ground-based physical measurement at a nearby location, we have been developing a procedure to derive solar resource data from photovoltaic (PV) performance data. Specifically, data such as measured by Enphase Energy Inc. micro-inverters, which have been deployed with millions of PV modules and have been providing reliable data with a 5-minute temporal resolution since 2011, and for some early systems since 2007.

The ac power, P_{ac} , data are used to back-solve for the unknown direct normal irradiance (DNI) and diffuse horizontal irradiance (DHI). The procedure required the development of two key methods: (1) determining the global tilted irradiance (GTI), otherwise known as the plane-of-array (POA) irradiance, from the P_{ac} , and (2) determining the DNI and DHI from the GTI. The DNI and DHI values (or their global horizontal irradiance (GHI) equivalent) may then be used with conventional modeling software, such as PVsyst, Helioscope, and NREL's System Advisor Model (SAM), to estimate the performance of PV systems of any size, or PV array tilt and azimuth orientation, including tracking.

The method to determine the DNI and DHI from the GTI was recently developed and published [1]. It is a modification of the DIRINT model by Perez et al. [2], which separates

input values of GHI into their DNI and DHI components. The modification substitutes GTI for GHI, and adds an iterative procedure to adjust the global clearness index to improve the derived values of DNI and DHI. The resulting model is referred to as the GTI-DIRINT model. The GTI-DIRINT model was validated using GTI values measured with Kipp & Zonen CMP11 and CMP22 pyranometers for three climatically diverse locations: Cocoa, Florida; Eugene, Oregon; and Golden, Colorado. For the GTI measured at a small tilt angle from the horizontal (10°), the deviations between the measured DNI and DHI and the GTI-DIRINT modeled DNI and DHI were essentially the same as those for the DIRINT model when using the GHI for model input. For larger tilt angles from horizontal, the deviations between modeled and measured values were larger, but still reasonable.

The method to determine the GTI from the P_{ac} was recently published [3]. It uses inverted PV performance models and solves a quadratic equation for the GTI from the input variables P_{ac} , wind speed, WS , dry bulb temperature, T_a , and the PV module temperature coefficients. A step was added to the GTI-DIRINT model to correct for the presence of angle-of-incidence (AOI) effects due to increased reflection losses from the PV module front cover when the AOI increases. This was accomplished within the GTI-DIRINT model iteration loop by correcting for AOI effects using a method for both direct beam and diffuse radiation [4].

The methods were developed using high quality data: GTIs measured with secondary standard pyranometers, P_{ac} measured with revenue grade meters ($\pm 0.2\%$ uncertainty), and WS and T_a measured on-site.

This work evaluated the methods when used with data that is more readily available for universal application of the method. For input values of P_{ac} , we used the micro-inverter data for the PV systems that were measured and archived by Enphase Energy Inc. For input values of T_a and WS , we used Automated Surface Observation Station (ASOS) data.

Results are presented for implementing the overall procedure to derive the DNI and DHI from the P_{ac} , and for then using the derived values of DNI and DHI to model the GTI and P_{ac} for the various tilted orientations.

II. DATA

We designed the validation experiment to include five identical PV module/Enphase Energy Inc. micro-inverter systems, each with a different tilt and azimuth orientation. Each of the five systems is instrumented to measure the P_{ac}



Fig. 1. PV modules with micro-inverters installed at NREL. Three PV modules are south-facing, with tilts of 10°, 25°, and 40° from the horizontal. A 4th PV module is tilted 40° and faces 30° west of south. A 5th PV module (not shown) is installed on a nearby two-axis tracker.

and GTI for comparison with the modeled values. The existing DNI and DHI measurements from the NREL's Solar Radiation Research Laboratory are also used for comparison with modeled values. The installed PV systems are shown in Fig. 1.

Non-NREL sources of data were used for input to the methods. For input values of P_{ac} , we used the micro-inverter data for the PV systems that were measured and archived by Enphase Energy Inc. under their Enlighten® program. For input values of T_a and WS , we used the Automated Surface Observation Station (ASOS) network data for the Broomfield, CO station. Broomfield is about 20 km northeast of NREL.

Data are 5-minute averages, except T_a and WS which were interpolated, from hourly data samples, to the midpoint of the 5-minute intervals. The data span the period April 1, 2014 through March 31, 2015.

Although the NREL and Enphase Energy Inc. data acquisition systems were measuring the same P_{ac} produced, differences in values occurred because of the measurement uncertainty, the 5-minute averaging methods, and the synchronization of the data acquisition clocks. The NREL P_{ac} measurements were made with a meter with an accuracy of $\pm 0.2\%$. The Enphase Energy Inc. P_{ac} measurements, due to economics being more important, have an accuracy of $\pm 2.5\%$.

Located between the micro-inverters and Enphase's Enlighten web-based monitoring and analysis software, hardware named Envoy is used for monitoring the performance of the micro-inverters and submitting the data to

Enlighten via the internet. At nominal 5-minute intervals, the Envoy sequentially polls each micro-inverter in the PV system to obtain the energy produced since last polled. Because the polling takes a second or so per micro-inverter, and the polling doesn't necessarily begin exactly at 5-minute increments past the hour, the polling for a micro-inverter could occur up to 2½ minutes from the 5-minute increments past the hour. The Envoy submits the energy produced to Enlighten after reappportioning the polled energy to evenly spaced 5-minute time stamps. For example, if the micro-inverter is polled at 13:07, two-fifths of the polled energy is included for the energy for the time stamp 13:05 and three-fifths of the polled energy is included for the energy for the time stamp 13:10. This preserves the integrity of the accumulated energy, but the result may differ from the NREL measured 5-minute averages when conditions are changing, such as due to cloud movement. (Enphase 5-minute energy values in joules were converted to average power in watts by dividing by 300 seconds.)

Clock synchronization also contributed to differences between Enphase and NREL measured 5-minute values of ac power. Although the Envoy submitted the micro-inverter data to Enlighten without a problem, NREL's internet security setting did not permit it to update its clock each day as intended, and this was not evident until after the measurement period when NREL had access to Enphase data. (Enlighten keeps track of when the clock is updated.) To agree closer to NREL data, the time stamps for the Enphase data were adjusted by 5 minutes, but a disagreement of up to 2 minutes likely still exists. A statistical comparison of the Enphase and NREL ac power data is provided in the next section.

III. RESULTS

Using the characteristic data for the PV systems; the Enphase Energy Inc. P_{ac} data; the ASOS T_a and WS data; values of DNI and DHI were derived for each of the three south-facing fixed-tilt PV systems. Each set of the derived DNI and DHI values were then used to model the performance (GTI and P_{ac}) of each of the five PV systems for the purpose of comparing the differences between the modeled and measured values.

Modeling results were evaluated using mean bias deviation (MBD) and root-mean-square deviation (RMSD) statistics, with the results expressed as a percent of the mean of the measured value. The deviation is the measured value subtracted from the modeled value. For the MBD, a positive value indicates that the model overestimates on average.

The means of the measured irradiance values are: DNI = 476 W/m²; DHI = 147 W/m²; GHI = 423 W/m²; GTI(10, 180) = 457 W/m²; GTI(25, 180) = 483 W/m²; GTI(40, 180) = 489 W/m²; GTI(40, 210) = 450 W/m²; and GTI(2X Trk) = 652 W/m²; where the GTI(*Tilt*, *Orientation*) notation of Vignola et al. [5] is used where *Tilt* is in degrees from horizontal and *Orientation* is the azimuth in degrees measured eastward from

true north. We designated the two-axis tracking orientation as GTI (2X Trk).

Using the same notation, the means of the ac power values measured by NREL are: $P_{ac}(10, 180) = 87.7$ W; $P_{ac}(25, 180) = 92.2$ W; $P_{ac}(40, 180) = 91.7$ W; $P_{ac}(40, 210) = 83.9$ W; and $P_{ac}(2X \text{ Trk}) = 122.9$ W.

For comparison, as appropriate, statistics were also determined for model efforts using measured values of DNI and DHI and modeled values of DNI and DHI determined with the DIRINT model.

A. Statistics for Enphase Measured P_{ac}

The P_{ac} values measured by Enphase were compared with the P_{ac} values measured by NREL to understand differences in the mean values reported (indicated by MBD) and the shorter term differences due primarily to averaging methods and time stamp errors from lack of regular clock synchronization (indicated by RMSD). The results are shown in Table 1. The MBDs for P_{ac} were 1.8% or less, which is within the stated uncertainty of 2.5% for the Enphase measurements. RMSDs were less than 10%.

TABLE 1

MEAN BIAS DEVIATION (MBD) AND ROOT-MEAN-SQUARE DEVIATION (RMSD) FOR ENPHASE MEASURED P_{ac} WHEN COMPARED TO NREL

MEASURED P_{ac}		
P_{ac}	MBD (%)	RMSD (%)
$P_{ac}(10, 180)$	1.1	7.4
$P_{ac}(25, 180)$	1.5	8.1
$P_{ac}(40, 180)$	1.8	7.9
$P_{ac}(40, 210)$	1.5	8.6
$P_{ac}(2X \text{ Trk})$	0.5	9.8

B. Statistics for Modeling DNI, DHI, and GHI

Using the P_{ac} values measured by Enphase, the GTIs were derived and then values of DNI and DHI were derived from the GTIs using the GTI-DIRINT model. The MBD and RMSD results, when using P_{ac} values for each of three south-facing fixed-tilt PV systems, are shown in Table 2. Also shown in

Table 2 are the results for the conventional approach of using the DIRINT model to derive DNI and DHI from a measured GHI. Results for determining the GHI from derived values of DNI and DHI are also provided for the application of the GTI-DIRINT model (not included when using the DIRINT model because the GHI is a model input).

Compared to DIRINT, the applications using GTI-DIRINT had similar MBDs and RMSDs for DHI and similar MBDs for DNI. The RMSDs for DNI were larger, but still reasonable considering that the RMSD from Table 1 for the Enphase measured P_{ac} likely propagated into the result. Also, because a GHI or GTI may result from many different combinations of DNI and DHI, the RMSDs for derived values of DNI and DHI are relatively large compared to modeling other parameters.

The MBDs for GHI were within about $\pm 1\%$. The RMSDs were a few percent larger than the RMSDs from Table 1 for the Enphase measured P_{ac} .

C. Statistics for Modeling GTIs Using the DNIs and DHIs

The DNI and DHI values from the preceding section were used with the Perez tilted surface model [6] to model the GTIs for the different PV module orientations. The MBD and RMSD results are shown in Table 3. As expected, using the measured values of DNI and DHI provided the best results, with MBDs within $\pm 1\%$ and RMSDs less than 8%. Next in performance was the DIRINT model when using measured values of GHI for model input, with MBDs within $\pm 1\frac{1}{2}\%$ and RMSDs less than 11%. When using the DNI and DHI values derived from the P_{ac} values for the various PV module orientations, MBDs were within $\pm 2\%$ and RMSDs were less than 18%. The MBDs of all methods are within the $\pm 3\%$ uncertainty of the GTI measurements.

D. Statistics for Modeling P_{ac}

The GTI values from the preceding section were used to model the P_{ac} for comparison with the NREL measured values of P_{ac} . The MBD and RMSD results are shown in Table 4. When using the GTIs determined from the measured values of DNI and DHI, the MBDs were within $\pm 2\frac{1}{2}\%$ and RMSDs were less than 10%.

TABLE 2

MEAN BIAS DEVIATION (MBD) AND ROOT-MEAN-SQUARE DEVIATION (RMSD) FOR DIRINT AND GTI-DIRINT MODELED VALUES OF DNI, DHI, AND GHI WHEN USING THE MEASURED GHI WITH DIRINT AND THE ENPHASE MEASURED P_{ac} WITH GTI-DIRINT FOR THE VARIOUS PV MODULE TILT AND AZIMUTH ORIENTATIONS.

Model/Input	DNI (mean = 476 W/m ²)		DHI (mean = 147 W/m ²)		GHI (mean = 423W/m ²)	
	MBD (%)	RMSD (%)	MBD (%)	RMSD (%)	MBD (%)	RMSD (%)
DIRINT/GHI	2.0	19.2	-5.1	35.1	----	----
GTI-DIRINT/						
$P_{ac}(10, 180)$	2.2	26.8	-3.9	38.0	1.2	10.6
$P_{ac}(25, 180)$	1.9	27.1	-3.6	38.1	0.9	10.9
$P_{ac}(40, 180)$	1.7	28.0	-4.3	37.8	0.2	11.7

TABLE 3

MEAN BIAS DEVIATION (MBD) AND ROOT-MEAN-SQUARE DEVIATION (RMSD) FOR MODELING THE GTI FOR THE DIFFERENT PV MODULE ORIENTATIONS WHEN USING THE MEASURED DNI AND DHI; THE DIRINT MODELED DNI AND DHI DERIVED FROM THE MEASURED GHI; AND THE GTI-DIRINT MODELED VALUES OF DNI AND DHI DERIVED FROM THE ENPHASE MEASURED P_{ac} FOR THE VARIOUS PV MODULE TILT AND AZIMUTH ORIENTATIONS.

Source for	GTI(10,180)		GTI(25,180)		GTI(40,180)		GTI(40,210)		GTI(2X Trk)	
	MBD (%)	RMSD (%)	MBD (%)	RMSD (%)	MBD (%)	RMSD (%)	MBD (%)	RMSD (%)	MBD (%)	RMSD (%)
Measured	-0.1	7.4	0.5	7.6	-0.1	7.9	0.1	8.4	0.9	7.5
DIRINT/GHI	0.0	7.4	0.7	8.0	0.2	8.7	0.2	9.5	1.4	10.6
GTI-DIRINT/ P_{ac} (10, 180)	1.4	9.1	2.2	9.6	1.6	10.0	1.7	11.1	2.0	15.7
P_{ac} (25, 180)	1.0	9.2	1.7	9.2	1.2	9.2	1.2	10.6	1.8	16.4
P_{ac} (40, 180)	0.2	10.0	0.8	9.5	0.2	9.2	0.3	10.8	1.6	17.8

TABLE 4

MEAN BIAS DEVIATION (MBD) AND ROOT-MEAN-SQUARE DEVIATION (RMSD) FOR MODELING THE P_{ac} FOR THE DIFFERENT PV MODULE ORIENTATIONS WHEN USING THE MEASURED DNI AND DHI; THE DIRINT MODELED DNI AND DHI DERIVED FROM THE MEASURED GHI; AND THE GTI-DIRINT MODELED VALUES OF DNI AND DHI DERIVED FROM THE ENPHASE MEASURED P_{ac} FOR THE VARIOUS PV MODULE TILT AND AZIMUTH ORIENTATIONS.

Source for	P_{ac} (10,180)		P_{ac} (25,180)		P_{ac} (40,180)		P_{ac} (40,210)		P_{ac} (2X Trk)	
	MBD (%)	RMSD (%)	MBD (%)	RMSD (%)	MBD (%)	RMSD (%)	MBD (%)	RMSD (%)	MBD (%)	RMSD (%)
Measured	-0.4	7.9	0.3	7.9	1.4	8.5	2.3	9.5	2.3	8.3
DIRINT/GHI	-0.3	7.9	0.5	8.2	1.7	9.3	2.4	10.5	2.8	11.5
GTI-DIRINT/ P_{ac} (10, 180)	1.1	7.4	1.9	8.3	3.1	9.5	3.9	11.0	3.3	16.5
P_{ac} (25, 180)	0.7	8.1	1.5	7.6	2.7	8.4	3.4	10.2	3.3	17.1
P_{ac} (40, 180)	-0.1	8.8	0.6	7.8	1.8	7.9	2.5	9.9	3.1	18.1

For the GTIs determined from DNI and DHI values from the DIRINT model and using measured values of GHI for model input, MBDs were within $\pm 3\%$ and RMSDs were less than 12%. When using the GTIs determined from DNI and DHI values derived from the Enphase P_{ac} values for the various PV module orientations, MBDs were within $\pm 4\%$ and RMSDs were less than 18%.

E. MBDs for Monthly P_{ac}

Fig. 2 shows the MBD by month for modeling the P_{ac} (40,180) when using: (a) the measured DNI and DHI; and (b) the DNI and DHI values derived from the Enphase measurements for the P_{ac} (25,180) orientation. Based on the work of Lee and Panchula [7], Fig. 2 includes an estimate of the MBD introduced due to spectral irradiance variations when using broadband DNI and DHI measurements to model the performance of a multi-crystalline PV module. The MBD related to spectral effects generally tracks the MBD for when using the measured DNI and DHI, indicating that it contributes to the variation in MBD by month for this method.

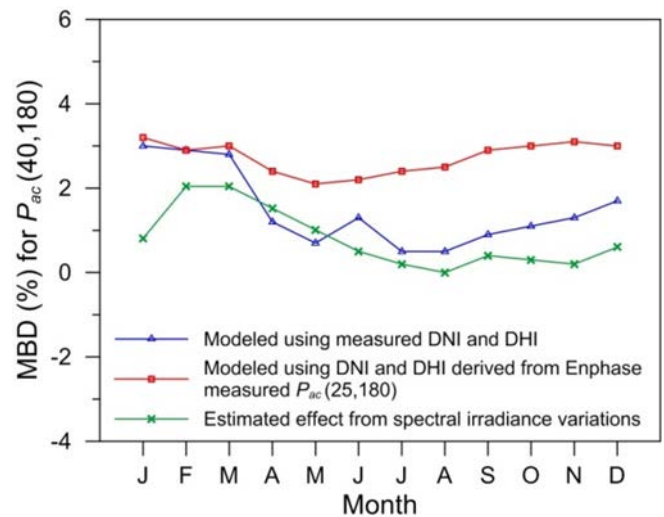


Fig. 2. Mean bias deviation (MBD) by month when modeling the P_{ac} (40,180) using: (a) the measured DNI and DHI; and (b) the DNI and DHI values derived from the Enphase measurements for the P_{ac} (25,180) orientation. The result using the measured DNI and DHI includes the estimated spectral effect. The result using the measured P_{ac} (25,180) shows less seasonal variability because spectral effects are automatically included, but does include the MBD of 1.5% from the Enphase measurement.

MBD variation by month when using the Enphase measurements is less because the spectral characteristics of the PV module used to derive the DNI and DHI values are essentially the same as for the PV module whose performance is modeled, but shows about a 1% increase in MBD from summer to winter. This may be a consequence of assumptions and estimates related to factors that impact seasonal performance, such as: temperature coefficient, PV module temperature, albedo, and AOI losses. When using the Enphase measurements, the MBD was also increased because of the presence of the MBD of the Enphase measurements (+1.5% from Table 1). Otherwise, the MBDs in Fig. 2 for this method would have been 1.5% less and more similar to the average of the method using the measured DNI and DHI.

IV. UNCERTAINTY ANALYSIS

The uncertainty of the method for predicting the annual P_{ac} was determined and quantified by the source element of the uncertainty. Sources of uncertainty were considered to be the bias type, but not the random type because the large number of data used to determine the annual P_{ac} serves to average out

random effects (more than 50,000 five-minute averages). The uncertainty of the method was also compared with other modeling methods using measured GHI and satellite derived GHI as the sources of the irradiance data. The results are shown in Table 5 and were determined as the root-sum-square of the elemental bias limits [8].

The overall bias limit for modeling the P_{ac} is $\pm 6.3\%$ when using the method using an Enphase measured P_{ac} , $\pm 7.1\%$ when using a satellite-based GHI, and $\pm 5.4\%$ when using a GHI measured with a well maintained secondary standard pyranometer.

Because the elements denoted by asterisks in Table 5 are used twice for the method using the Enphase measured P_{ac} , once when deriving the DNI and DHI from the measured P_{ac} and again when using the derived DNI and DHI to model the P_{ac} of another PV system, their elemental bias limits are greater by a factor of the square root of two than for the other methods. These elements are generally associated with the PV module and inverter specifications. Smaller bias limits were used for elements where the method compensates for their effect. These elements include the spectral effect and soiling.

TABLE 5

UNCERTAINTY ELEMENTS FOR MODELING THE ANNUAL P_{AC} FOR THE VARIOUS METHODS.

Element	Method for Modeling the P_{ac}		
	Measured GHI, DIRINT Model, Perez Tilted Surface Model Bias Limit ($\pm\%$)	Satellite GHI, DIRINT Model, Perez Tilted Surface Model Bias Limit ($\pm\%$)	Enphase Measured P_{ac} , GTI-DIRINT Model, Perez Tilted Surface Model Bias Limit ($\pm\%$)
GHI	2.0	5.0	-
Enphase measured P_{ac}	-	-	2.5
PV module power rating	3.0	3.0	4.2*
PV module binning	1.0	1.0	1.4*
DIRINT model + Perez tilted surface model	1.5	1.5	-
GTI-DIRINT model + Perez tilted surface model	-	-	1.5
Spectral effect	1.8	1.8	0.5
Irradiance effect	1.0	1.0	1.4*
AOI effect	0.5	0.5	0.7
Temperature effect			
γ bias limit $\pm 7.5\%$	0.8	0.8	1.1*
ASOS location	1.0	1.0	1.4*
Temperature model	1.2	1.2	1.7*
Inverter model	1.0	1.0	1.4*
Inverter clipping	-	-	1.0
Soiling estimate	2.0	2.0	0.5
Root-sum-square of the elemental bias limits	5.4	7.1	6.3

*These bias limits are a factor of the square root of two or 1.4 greater than for the other two methods because they are used twice, once when deriving the DNI and DHI from the measured P_{ac} and again when using the derived DNI and DHI to model the P_{ac} of another PV system.

V. SUMMARY

Using PV performance data from PV modules with micro-inverters affords the opportunity to provide ground-based solar resource values of DNI and DHI critical for developing PV projects. From the measured P_{ac} , values of DNI and DHI were derived, and then used to model the performance of other PV modules with micro-inverters with different azimuth and tilt orientations. The annual MBDs were within $\pm 4\%$, and only 1% greater than when the PV performance was modeled using high quality irradiance measurements. An uncertainty analysis shows the method's uncertainty for modeling the annual ac energy for a PV system to be $\pm 6.3\%$, which is less than the $\pm 7.1\%$ uncertainty when modeling the PV performance using satellite-based global horizontal irradiance data

ACKNOWLEDGEMENT

This work was supported by the U.S. Department of Energy under Contract No. DE-AC36-08-GO28308 with the National Renewable Energy Laboratory (NREL). Funding provided by U.S. DOE Office of Energy Efficiency and Renewable Energy Solar Energy Technologies Program. The authors are thankful for the efforts of Bill Sekulic, Jose Rodriguez, and Greg Perrin at NREL, who performed the irradiance and PV performance measurements.

The U.S. Government retains and the publisher, by accepting the article for publication, acknowledges that the U.S. Government retains a nonexclusive, paid-up, irrevocable,

worldwide license to publish or reproduce the published form of this work, or allow others to do so, for U.S. Government purposes.

REFERENCES

- [1] B. Marion, "A model for deriving the direct normal and diffuse horizontal irradiance from the global tilted irradiance", *Solar Energy* 122: 1037–1046, 2015.
- [2] R. Perez, P. Ineichen, E. Maxwell, R. Seals, A. Zelenka, "Dynamic global-to-direct irradiance conversion models", In: ASHRAE Transactions-Research Series, 354–369, 1992.
- [3] B. Marion, B. Smith, "Photovoltaic system derived data for determining the solar resource and for modeling the performance of other photovoltaic systems", *Solar Energy* 147: 349–357, 2017.
- [4] B. Marion, "Numerical method for angle-of-incidence correction factors for diffuse radiation incident photovoltaic modules", *Solar Energy* 147: 344–348, 2017.
- [5] F. Vignola, J. Michalsky, T. Stoffel, *Solar and infrared radiation measurements*, CRC Press, Boca Raton, 2012.
- [6] R. Perez, P. Ineichen, R. Seals, J. Michalsky, "Modeling daylight availability and irradiance components from direct and global irradiance", *Solar Energy* 44: 271–289, 1990.
- [7] M. Lee, A. Panchula, "Spectral correction for photovoltaic module performance based on air mass and precipitable water", in 43rd IEEE PVSC, 2016.
- [8] R. Dieck, *Measurement Uncertainty—Methods and Application*, Instrument Society of America: Research Triangle Park, 1992.